Landscape phenology and soil moisture dynamics influenced by irrigation in a desert urban environment

Chenghao Wang
Stanford University, Stanford, USA
chenghao.wang@stanford.edu

Abstract: Natural vegetation in arid and semi-arid environments is usually water-limited, while the urbanization process alters its phenology through anthropogenic activities such as irrigation and fertilization. In particular, urban irrigation has also been used as one of the strategies to alleviate heat stress during hot seasons. In this study, we aim to examine the impacts of irrigation and its scheduling on vegetation phenology and soil moisture dynamics in the Phoenix Metropolitan Area, a desert urban environment located in Arizona. We first investigate the plant phenology over different land cover types based on long-term remotely sensed data. Results show that precipitation is the primary determinant of natural vegetation growth, while irrigation controls urban greening and agricultural phenology. We then evaluate different irrigation schedules use a soil water balance model. Simulations suggest that irrigation substantially reduces plant water stress, but its effect varies with the scheduling. Seasonally varied daily irrigation is identified as the optimal irrigation practice to reduce plant water stress and improve evapotranspiration for both urban vegetation and crops. This study highlights the critical role irrigation plays in vegetation phenology in arid and semi-arid environments, and sheds new light on effectively using irrigation to mitigate heat stress in a desert city.

Keywords: Vegetation phenology; urban irrigation scheduling; soil water dynamics; plant water stress.

1. Introduction

Available water and energy input are essential to the functioning of vegetation, especially in extreme environments (Schwinning *et al.*, 2004). For arid and semi-arid ecosystems, precipitation is the major available water resource, which significantly influences the dynamics of vegetation (Snyder and Tartowski, 2006). The timing, frequency, and magnitude of precipitation are crucial to the vegetation growth via the interactions of climate–soil–vegetation system (Laio *et al.*, 2001; Ogle and Reynolds, 2004). Heisler-White *et al.*, (2008) evaluated the response of aboveground net primary productivity (ANPP) of semi-arid grasslands to the increasing precipitation event size, and suggested that the ANPP would increase with fewer but larger rainfall events. Another study on three North American deserts showed the sensitivity of net ecosystem CO_2 exchange to rainfall event size (Huxman *et al.*, 2004).

In contrast, anthropogenic activities bring in exotic vegetation during the urbanization process, and the phenology of these species can be distinct from those living in the natural environment (Verdugo-

Imaginable Futures: Design Thinking, and the Scientific Method. 54th International Conference of the Architectural Science Association 2020, Ali Ghaffarianhoseini, et al (eds), pp. 670–679.

Vásquez *et al.*, 2016). For example, irrigation as the additional water input increases the water availability, while fertilization in agricultural development improves the primary productivity of crops. A study of deciduous broadleaf forest over the Eastern United States showed that urban vegetation has a growing season 8 days longer than the surrounding forest (White *et al.*, 2002). In the arid Phoenix Metropolitan Area, studies have found distinct vegetation growth multimodality within agricultural and urban areas when compared to that in the surrounding desert (Buyantuyev and Wu, 2012; Zhang *et al.*, 2020).

To evaluate the vegetation phenology and its response to climate and land cover changes, experiments and numerical simulations have been conducted (e.g., Laio *et al.*, 2001). However, in situ measurements have limited spatial and temporal coverages, while numerical simulations are not capable of fully capturing the land–atmosphere interactions. Remote sensing techniques provide an alternative and attractive means to assess the long-term changes of vegetation via proxies such as the Normalized Difference Vegetation Index (NDVI) and the Enhanced Vegetation Index (EVI). For instance, NDVI has been used to study surface moisture, water deficit, and crop water use (Schnur *et al.*, 2010).

In this study, we evaluate the vegetation phenology under different land cover conditions, i.e., urban, agricultural, and natural desert land covers (shrubland and grassland), using a 15-year record of remotely sensed NDVI and EVI over the Phoenix Metropolitan Area. A soil water balance model is modified to incorporate irrigation and EVI-driven plant seasonal variability. Four irrigation schedules are selected to numerically examine the responses of soil moisture dynamics and plant water stress to additional water input. This study aims to answer the following questions: (i) how vegetation seasonality differs under various land cover conditions, (ii) whether rainfall is the driver the vegetation growth for different land covers, and (iii) how irrigation schedules regulate soil moisture dynamics and plant water stress.

2. Data collection and methodology

2.1. Data sources

We retrieved the 30-m National Land Cover Database (NLCD) products for 2001, 2006, and 2011 (https://www.mrlc.gov/data) over the Phoenix Metropolitan Area. NLCD datasets have 16 land cover types over the contiguous United States, with four different urban land cover types ranging from open space to high intensity. Here we consider Shrub/Scrub, Grassland/Herbaceous, and Cultivated Crops in NLCD's classification system as (natural) shrubland, grassland, and agricultural area, respectively. Figure 1 shows the NLCD 2011 product over Phoenix (as an example) and the satellite images of typical landscapes. We also retrieved the 500-m Moderate Resolution Imaging Spectroradiometer (MODIS) MCD12Q1 Version 5 product (2001–2013) with the IGBP global vegetation classification scheme (Friedl *et al.*, 2010). However, large discrepancies exist between NLCD and MCD23Q1 datasets. For example, the urban area in MCD12Q1 remains intact for 13 years, while the Phoenix Metropolitan Area has undergone extensive urban growth during the past two decades (Wang and Wang, 2017). NLCD products are therefore considered more reliable and are used in the following analyses. We further resampled 30-m NLCD products to a coarser resolution of 250 m.

Two vegetation indices, i.e., NDVI and EVI, during 2001–2015 were retrieved from 16-day MODIS vegetation indices Version 6 product (MOD13Q1) (https://lpdaac.usgs.gov/products/mod13q1v006/). The spatial resolution of this product is 250 m. Note that NDVI is more sensitive to chlorophyll, while EVI is more sensitive to canopy structural variations such as leaf area index and canopy architecture (Huete

et al., 2002). We removed pixels with invalid vegetation indices data and derived the time series of spatial averages over the same land cover type. The NDVI and EVI values over 7 different land cover types during 2001–2005, 2006–2010, and 2011–2015 are based on NLCD 2001, 2006, and 2011 products, respectively.

We use meteorological data (1) to derive precipitation parameters for the point-scale soil water balance model, and (2) to determine the irrigation amount and scheduling. Daily precipitation data in 2001–2015 at the Phoenix Sky Harbor International Airport were downloaded from the National Climatic Data Center's Climate Data Online website (https://www.ncdc.noaa.gov/cdo-web/). Two Arizona Meteorological (AZMET) Network stations, i.e. Buckeye and Phoenix Encanto, were selected as examples of agricultural land and urban areas, respectively. Figure 1 shows the locations of these three stations and their surrounding environment (satellite images). Note that the Phoenix Encanto station is located on the Encanto Golf Course. The reference evapotranspiration (ET_{os}) data during 2003–2015 were used to calculate the maximum vegetation evapotranspiration by including crop coefficients (K_c) (Brown, 2005).

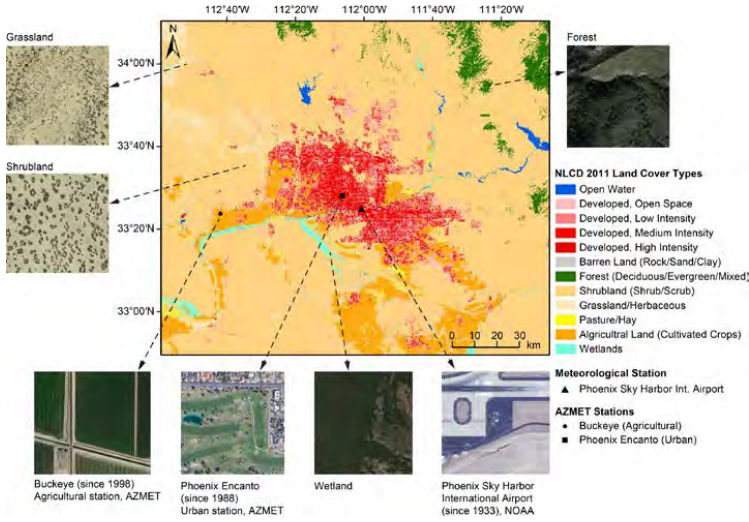

Figure 1: NLCD 2011 map, satellite images of typical landscapes (source: Google Earth Pro in 2017), and the geographical locations of NOAA Phoenix Airport station and two AZMET stations.

2.2. Point-scale soil water balance model

A modified point-scale soil water balance model originally developed by Laio *et al.*, (2001) is used to simulate the change of relative soil moisture *s* over time *t* for one representative natural land cover type (shrubland) as well as agricultural and urban lands by including irrigation effect,

$$nZ_r \frac{ds}{dt} = P(t) + Irr(t) - I(t) - Q(s,t) - \mathrm{ET}(s,t) - L(s,t), \quad (1)$$

where n is the soil porosity, Z_r the rooting depth (the depth of active soil), P the precipitation, Irr the irrigation, I the interception, Q the runoff, ET the evapotranspiration, and L the leakage (all in LT^{-1}). The first three terms on the right-hand side of Eq. 1 represent the available rainfall and irrigation that reach the soil, while the last three terms constitute water losses.

Precipitation input can be regarded as independent from the soil moisture state at the point scale (Laio *et al.*, 2001). The rainfall series is treated as a series of point events over time and can be simulated as a stochastic Poisson process with a mean arrival rate λ (day^{-1}) and a mean storm/event depth α (mm). Note that λ is the reciprocal of the mean arrival time of the rainfall pulses ($1/\lambda$, unit: day). These two parameters are derived based on measurements at the Phoenix Airport station (2001–2015), and can be used to generate rainfall series that follows the distribution of observations.

Interception I is simplified as a parameter that depends on vegetation. Without irrigation, infiltration happens only if the precipitation amount is higher than interception. Runoff Q is considered as saturation excess runoff, and it occurs when $s > 1$. ET is treated as a piecewise function with four stages

$$\mathrm{ET}(s,t) = \begin{cases} 0, & s \le s_h \\ E_w \dfrac{s - s_h}{s_w - s_h}, & s_h < s \le s_w \\ E_w + (\mathrm{ET}_{\max} - E_w)\dfrac{s - s_w}{s^* - s_w}, & s_w < s \le s^* \\ \mathrm{ET}_{\max}, & s^* < s \le 1 \end{cases}, \quad (2)$$

where s_h, s_w, and s^* are hygroscopic point, wilting point, and plant water stress threshold, respectively, and E_w and $\mathrm{ET}_{\max}$ are the bare soil evaporation rate at s_w and the maximum ET rate when s is greater than the stress threshold, respectively.

Leakage L is described as the decrease of the hydraulic conductivity K over time as soil dries out,

$$L(s,t) = K(s,t) = K_s \frac{e^{\beta(s - s_{fc})} - 1}{e^{\beta(1 - s_{fc})} - 1}, \quad (3)$$

where K_s is the saturated hydraulic conductivity at $s = 1$, and $\beta = 2b + 4$. Here b is the pore size distribution index. The hydraulic conductivity decreases to zero at the field capacity s_{fc}.

The static plant water stress ζ is evaluated as (Porporato *et al.*, 2001)

$$\zeta(s,t) = \left[\frac{s^* - s}{s^* - s_w}\right]^q, \quad (4)$$

for $s_w \le s \le s^*$, where q measures the nonlinearity of the soil moisture deficit impacts on plant conditions. Here $q = 3$ is assumed (Porporato *et al.*, 2001). Note that $\zeta = 0$ when $s > s^*$, while the plant water stress reaches its maximum when s drops below wilting point ($s < s_w$).

Urban vegetation in this study is assumed to be turfgrass. Here two types of grass species are considered. During the summer (May–September) bermudagrass is the only grass species, while the

practice of overseeding with ryegrass is conducted in October (Brown, 2003; Kopec and Umeda, 2015). The presence of ryegrass lasts from October to April next year. The ET_{max} of both species over time can be estimated using the measured ET_{os} at the Phoenix Encanto station, the appropriate crop coefficients (K_c) (Brown, 2003), and an EVI reduction coefficient, f, as

$$ET_{max}(t) = ET_{os}(t) \times K_c(t) \times f(\text{EVI}, t). \quad (5)$$

The EVI reduction coefficient incorporates plant seasonality based on remotely sensed vegetation index,

$$f(\text{EVI}, t) = \text{EVI}(t) / \text{EVI}_{max}, \quad (6)$$

where EVI(t) is the mean monthly EVI over low intensity urban areas, while EVI_{max} is the maximum of 12 monthly EVI values. Such approach is informed by the strong relationship between vegetation indices and ET (Glenn *et al.*, 2008). For urban vegetation, monthly series of $ET_{os}(t)K_c(t)$ are used based on high quality turf data in Brown's (2003) study. For months with EVI_{max}, the interception I_{max} by grass is assumed to be 1.0 mm day^{-1} (Zhou *et al.*, 2013). For other months, the interception is determined as

$$I(t) = I_{max} \times f(\text{EVI}, t). \quad (7)$$

The maximum rooting depth $Z_{rmax,ber}$ for bermudagrass during its active period (May–September) is 150 mm (Cardenas-Lailhacar *et al.*, 2010), while $Z_{rmax,rye}$ for ryegrass during its active period (October–April) is 70 mm (Wedderburn *et al.*, 2010). The varying $Z_{r,ber}$ and $Z_{r,rye}$ for other months are calculated as

$$Z_{r,ber} = Z_{rmax,ber} \times f_{ber}(\text{EVI}, t), \quad (8)$$

$$Z_{r,rye} = Z_{rmax,rye} \times f_{rye}(\text{EVI}, t), \quad (9)$$

and the reduction coefficients are

$$f_{ber}(\text{EVI}, t) = \text{EVI}(t) / \text{EVI}_{max,May–Sep}, \quad (10)$$

$$f_{rye}(\text{EVI}, t) = \text{EVI}(t) / \text{EVI}_{max,Oct–Apr}, \quad (11)$$

where $EVI_{max,May–Sep}$ and $EVI_{max,Oct–Apr}$ are maximum values of monthly mean EVI during the growing periods of bermudagrass and ryegrass, respectively.

Crops over agricultural land experience rotation every year. Here we assume crops to be cotton in April–October and durum wheat in November–April (most widely harvested in Arizona) (USDA, 1997). Crop coefficients for two species are based on the guidelines of Food and Agriculture Organization (Allen *et al.*, 1998). Calculations of monthly ET_{max} and I follow Eqs. 5–7 using EVI over agricultural lands, while ET_{os} is based on the Buckeye station. The maximum interception is assumed to be 1 mm day^{-1}. The maximum rooting depths of cotton and durum wheat during their active periods are 1220 mm and 2000 mm, respectively, based on previous studies (Grimes *et al.*, 1975; Gregory *et al.*, 1978). Varying rooting depths in other months can then be determined using reduction coefficients as in Eqs. 10–11.

Creosotebush is selected as the example species for shrubland (Hartman, 1977). The crop coefficients for creosotebush are from Neale *et al.* (2011). ET_{os} data when using Eq. 5 are from the Buckeye station as AZMET has no rural stations. Monthly ET_{max} values are further scaled following Schreiner-McGraw *et al.* (2016). Here EVI data over shrubland are used, and the maximum interception is assumed to be 1.5 mm day^{-1} (Zhou *et al.*, 2013). The maximum rooting depth is 2000 mm (Gibbens and Lenz, 2001). Similar EVI reduction coefficients are also used.

Uniform soil texture of sandy loam (Hartman, 1977) is used here, and the soil parameters follow Laio *et al.* (2001): n = 0.43, s_h = 0.14, s_w = 0.18, s^* = 0.46, s_{fc} = 0.56, b = 4.90, and K_s = 800 mm day^{-1}. We aim to evaluate *on average* the responses of soil moisture dynamics and plant water stress to precipitation and irrigation. Therefore, for each land cover with or without irrigation, numerical simulations of continuous 1000 years were performed, and results are evaluated based on monthly or annual averages.

2.3. Irrigation scheduling

The irrigation amount needed for urban areas and agricultural land is estimated to be equal to the ET_{max} throughout the year. As a result, the annual irrigation amount needed for urban vegetation (1397.2 mm) is slightly lower than that for agriculture (1671.4 mm). Similar to Volo *et al.* (2014), four irrigation scenarios are designed, i.e., daily constant (DC), daily seasonal (DS), monthly constant (MC), and monthly seasonal (MS), with identical annual irrigation amount but different frequency and size of delivery (Figure 2). The responses of soil moisture dynamics and plant water stress can reveal the optimal irrigation scheduling using the soil water balance model.

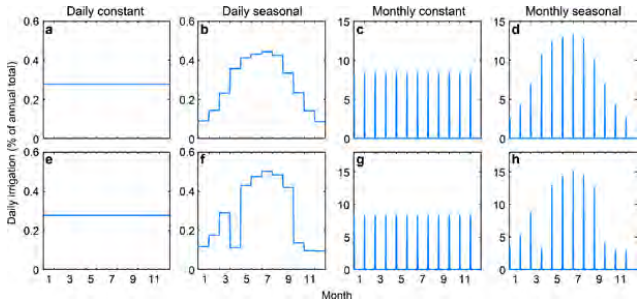

Figure 2: Different irrigation scheduling for (a–d) urban areas and (e–h) agricultural land.

3. Results and discussion

3.1. Vegetation phenology based on remotely sensed vegetation indices

Figure 3b and c shows the average 16-day NDVI and EVI over time under seven land cover conditions during 2001–2015. Winter and monsoon seasons with precipitation higher than 100 mm are shaded in blue and red, respectively. The spatial and temporal patterns of NDVI and EVI are in general consistent, although NDVI is relatively higher than EVI. Grassland has the highest coefficient of variation (CV = 0.29 for NDVI) among all land cover types, although its mean NDVI (or EVI) is relatively low, suggesting its high sensitivity to precipitation. Similarly, shrubland has the second largest CV with mean NDVI (or EVI) relatively higher than that of grassland. Agricultural land has the highest vegetation index level. The mean NDVI or EVI over open space, low intensity, and high intensity urban areas is close to that over shrubland, while high intensity urban areas have the lowest NDVI or EVI level. In addition, the CVs of NDVI and EVI over agricultural land and urban areas are much smaller than those of natural landscape, suggesting that the phenology of agricultural and urban vegetation is not determined by precipitation. Instead, irrigation is the predominant water input over these areas. The highest NDVI or EVI peaks over natural landscapes are observed mainly during winters and springs with high seasonal rainfalls (Figure 3).

In contrast, large monsoonal rainfalls have limited impact on natural vegetation, possibly because the water input is insufficient to support growth when ET rate is very high during hot summers (see Section 3.2).

Figure 3e shows monthly EVI in the study area. The annual multimodality of EVI is clear for most land cover types. The two peaks of EVI result from crop rotation and repeated urban grass overseeding practice. Natural desert vegetation usually has only one growing season which often ends during the pre-summer drought. EVI over natural landscapes is also controlled by the precipitation peak in March, although the EVI peak is one month later than the winter rainfall peak as limited by temperature. Summer rainfalls have relatively marginal impacts on vegetation growth over natural landscapes, but can further improve the growth of irrigation-fed vegetation in urban and agricultural areas.

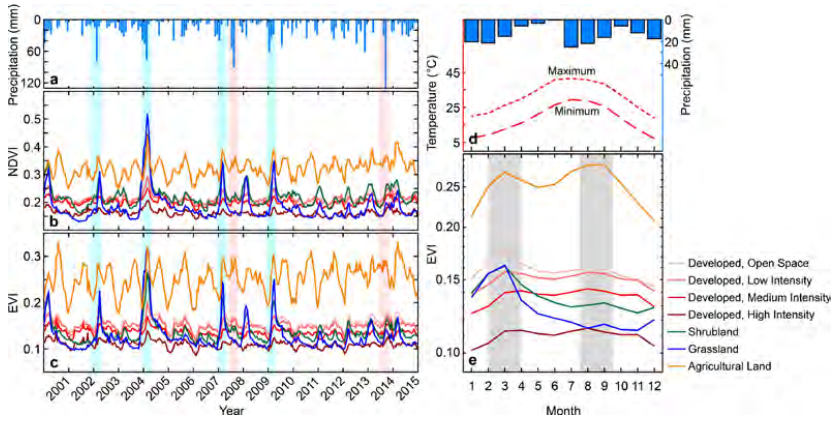

Figure 3: Long-term (a) monthly precipitation and 16-day (b) NDVI and (c) EVI, as well as monthly mean (d) precipitation, (e) temperature, and EVI in the Phoenix Metropolitan Area. Note that precipitation and temperature are observations from the Phoenix Airport station.

3.2. Responses of soil moisture dynamics and plant water stress to precipitation and irrigation

Figure 4 shows the simulated soil moisture dynamics and plant water stress under natural condition (without irrigation). For all three land cover types, the lowest soil moisture and the highest static water stress occur in the pre-monsoon season owing to high temperature and low precipitation. The mean soil moisture content is below the wilting point in most months, suggesting extremely high water stress. With a shallower rooting depth, urban grass has the highest mean soil moisture during monsoon (summer) and winter seasons. The bimodality of ET is in line with NDVI or EVI observations and growing seasons. Surface runoff and leakage occur in some months for urban grass, while for shrubland and agricultural land, precipitation is completely converted to ET. The leakage amount of urban grass is much greater than runoff, especially in winter. In contrast, limited leakage and runoff are observed in summer due to the high demand of ET. The probability distribution function (pdf) of static water stress shows that plants over all three land cover types, if without irrigation, are under high water stress (mean

ζ > 0.9). With a shallow rooting depth, the ζ of urban grass can drop to zero during large rainfall events. The highest ET_{max} during most months over agricultural areas results in the highest mean static water stress.

Figure 5 shows the responses of soil moisture to different irrigation schedules. Compared to natural conditions, irrigation substantially alleviates plant water stress and elevates mean soil moisture. For urban areas, irrigating only once per month (monthly pulses) results in higher plant water stress and lower mean soil moisture than daily irrigation. Note that the two monthly irrigation practices have nearly identical patterns of soil moisture. The constant urban daily irrigation throughout the year yields the lowest mean static water stress and highest mean soil moisture (0.36), although its *s* during summer is lower than that with seasonally varied daily irrigation (Volo *et al.*, 2014). The impact of irrigation on reducing crop water stress is even more significant than over urban areas, as suggested by the lower mean ζ values. The seasonally varied daily irrigation leads to the lowest mean static water stress. The soil moisture in two constant scenarios is higher than s_{fc} during winter.

We further examine the partitioning of available water. Among the four urban irrigation practices, daily seasonal scenario yields the maximum ET amount (74.8% of annual water input) with only marginal leakage loss (2.2% of annual water input). In contrast, a large portion of available water (63.6%) in two urban monthly scenarios is converted to runoff. The daily seasonal scenario for agricultural irrigation also has the maximum ET amount (81.7% of the annual water input). As the net primary productivity is closely related to ET amount (Churkina *et al.*, 1999), the daily seasonal scenario is considered as the optimal practice for both urban areas and agricultural land.

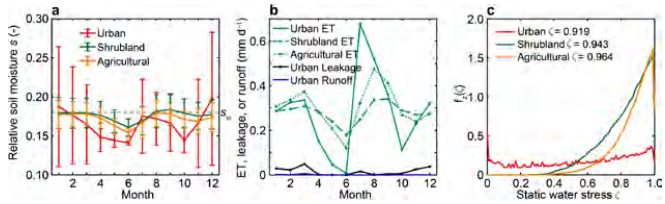

Figure 4: (a) Monthly relative soil moisture content, (b) monthly ET, leakage, and runoff, and (c) probability distribution functions $f_z(\zeta)$ of static water stress (probability for ζ = 0 and 1 not shown) under natural condition (no irrigation). Error bars in (a) show standard deviation of 1000-year simulations, while ζ values in (c) show the mean values.

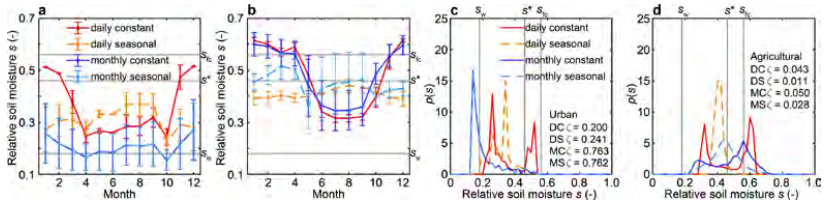

Figure 5: Monthly relative soil moisture content and pdfs of *s* for four irrigation schedules over (a) and (c) urban area, and (b) and (d) agricultural land. Note that ζ values in (c) and (d) are the mean values (DC = daily constant, DS = daily seasonal, MC = monthly constant, and MS = monthly seasonal).

4. Concluding remarks

In this study, we examine the vegetation phenology under different land cover conditions in the Phoenix Metropolitan Area using long-term remotely sensed data. Results suggest that agricultural land has the highest mean NDVI or EVI, followed by urban areas with low intensity and open space, both due to irrigation practices. In contrast, natural shrubland and grassland have relatively low mean NDVI or EVI levels as limited by available water, with high sensitivity to precipitation. Winter rainfall is the major driver of the peak vegetation growth over shrubland, while the strong bimodality in agriculture and urban areas results from crop rotation, repeated grass overseeding practice, and irrigation. Simulations using a modified soil water balance model show that with the same annual irrigation amount, seasonally varying daily irrigation is the optimal practice to reduce plant water stress and promote plant growth in both urban areas and agricultural land. This study also has strong implications for urban planning of effectively using irrigation to mitigate heat stress during hot seasons. Arid cities like Phoenix should also pay attention to the trade-off between water use and heat mitigation (Wang *et al.*, 2019).

Acknowledgements

The author thanks Dr. Enrique R. Vivoni and two anonymous reviewers for their constructive comments.

References

Allen, R.G., Pereira, L.S., Raes, D. and Smith, M. (1998) Crop evapotranspiration - Guidelines for computing crop water requirements-FAO Irrigation and drainage paper 56, *FAO, Rome*, 300(9), p. D05109.

Brown, P.W. (2003) *Turfgrass consumptive use values for the Phoenix area*. AZ1314. Tucson, Arizona: The University of Arizona.

Brown, P.W. (2005) *Standardized reference evapotranspiration: A new procedure for estimating reference evapotranspiration in Arizona*. AZ1234. Tucson, Arizona: The University of Arizona.

Buyantuyev, A. and Wu, J. (2012) Urbanization diversifies land surface phenology in arid environments: Interactions among vegetation, climatic variation, and land use pattern in the Phoenix metropolitan region, USA, *Landscape and Urban Planning*, 105(1–2), 149–159.

Cardenas-Lailhacar, B., Dukes, M.D. and Miller, G.L. (2010) Sensor-based automation of irrigation on bermudagrass during dry weather conditions, *Journal of Irrigation and Drainage Engineering*, 136(3), 184–193.

Churkina G., Running, S.W. and Schloss, A.L. (1999) Comparing global models of terrestrial net primary productivity (NPP): the importance of water availability, *Global Change Biology*, 5, 46–55.

Friedl, M.A., Sulla-Menashe, D., Tan, B., Schneider, A., Ramankutty, N., Sibley, A. and Huang, X. (2010) MODIS Collection 5 global land cover: Algorithm refinements and characterization of new datasets, *Remote Sensing of Environment*, 114(1), 168–182.

Gibbens, R.P. and Lenz, J.M. (2001) Root systems of some Chihuahuan Desert plants, *Journal of Arid Environments*, 49(2), 221–263.

Glenn, E.P., Huete, A.R., Nagler, P.L. and Nelson, S.G. (2008) Relationship between remotely-sensed vegetation indices, canopy attributes and plant physiological processes: What vegetation indices can and cannot tell us about the landscape, *Sensors*, 8(4), 2136–2160.

Gregory, P., McGowan, M., Biscoe, P. and Hunter, B. (1978) Water relations of winter wheat: 1. Growth of the root system, *The Journal of Agricultural Science*, 91(1), 91–102.

Grimes, D.W., Miller, R.J. and Wiley, P.L. (1975) Cotton and corn root development in two field soils of different strength characteristics, *Agronomy Journal*, 67(4), 519–523.

Hartman, G.W. (1977) *Soil survey of Maricopa County, Arizona, central part*. Department of Agriculture, Soil Conservation Service.

Heisler-White, J. L., Knapp, A. K. and Kelly, E. F. (2008) Increasing precipitation event size increases aboveground net primary productivity in a semi-arid grassland, *Oecologia*, 158(1), 129–140.

Huete, A., Didan, K., Miura, T., Rodriguez, E.P., Gao, X. and Ferreira, L.G. (2002) Overview of the radiometric and biophysical performance of the MODIS vegetation indices, *Remote Sensing of Environment*, 83(1), 195–213.

Huxman, T.E., Snyder, K.A., Tissue, D., Leffler, A.J., Ogle, K., Pockman, W.T., Sandquist, D.R., Potts, D.L. and Schwinning, S. (2004) Precipitation pulses and carbon fluxes in semiarid and arid ecosystems, *Oecologia*, 141(2), 254–268.

Kopec, D. and Umeda, K. (2015) *Overseeding winter grasses into bermudagrass turf*. AZ1683. Tucson, Arizona: The University of Arizona.

Laio, F., Porporato, A., Ridolfi, L. and Rodriguez-Iturbe, I. (2001) Plants in water-controlled ecosystems: active role in hydrologic processes and response to water stress: II. Probabilistic soil moisture dynamics, *Advances in Water Resources*, 24(7), 707–723.

Neale, C.M.U., Geli, H., Taghvaeian, S., Masih, A., Pack, R.T., Simms, R.D., Baker, M., Milliken, J.A., O'Meara, S. and Witherall, A.J. (2011) Estimating evapotranspiration of riparian vegetation using high resolution multispectral, thermal infrared and lidar data, in *Remote Sensing for Agriculture, Ecosystems, and Hydrology XIII*, 81740P.

Ogle, K. and Reynolds, J.F. (2004) Plant responses to precipitation in desert ecosystems: integrating functional types, pulses, thresholds, and delays, *Oecologia*, 141(2), 282–294.

Porporato, A., Laio, F., Ridolfi, L. and Rodriguez-Iturbe, I. (2001) Plants in water-controlled ecosystems: active role in hydrologic processes and response to water stress: III. Vegetation water stress, *Advances in Water Resources*, 24(7), 725–744.

Schnur, M.T., Xie, H. and Wang, X. (2010) Estimating root zone soil moisture at distant sites using MODIS NDVI and EVI in a semi-arid region of southwestern USA, *Ecological Informatics*, 5(5), 400–409.

Schreiner-McGraw, A.P., Vivoni, E.R., Mascaro, G. and Franz, T.E. (2016) Closing the water balance with cosmic-ray soil moisture measurements and assessing their relation to evapotranspiration in two semiarid watersheds, *Hydrology and Earth System Sciences*, 20(1), 329–345.

Schwinning, S., Osvaldo, E.S., Loik, M.E. and Ehleringer, J.R. (2004) Thresholds, memory, and seasonality: understanding pulse dynamics in arid/semi-arid ecosystems, *Oecologia*, 141(2), 191–193.

Snyder, K.A. and Tartowski, S.L. (2006) Multi-scale temporal variation in water availability: Implications for vegetation dynamics in arid and semi-arid ecosystems, *Journal of Arid Environments*, 65(2), 219–234.

USDA (1997) *Usual planting and harvesting dates for US field crops*. Agricultural Handbook Number 628. National Agricultural Statistics Service.

Verdugo-Vásquez, N., Acevedo-Opazo, C., Valdés-Gómez, H., Araya-Alman, M., Ingram, B., de Cortázar-Atauri, I.G. and Tisseyre, B. (2016) Spatial variability of phenology in two irrigated grapevine cultivar growing under semi-arid conditions, *Precision Agriculture*, 17(2), 218–245.

Volo, T. J., Vivoni, E.R., Martin, C.A., Earl, S. and Ruddell, B.L. (2014) Modelling soil moisture, water partitioning, and plant water stress under irrigated conditions in desert urban areas, *Ecohydrology*, 7(5), 1297–1313.

Wang, C. and Wang, Z.-H. (2017) Projecting population growth as a dynamic measure of regional urban warming, *Sustainable Cities and Society*, 32, 357–365.

Wang, C., Wang, Z.-H. and Yang, J. (2019) Urban water capacity: Irrigation for heat mitigation, *Computers, Environment and Urban Systems*, 78, 101397.

Wedderburn, M.E., Crush, J.R., Pengelly, W.J. and Walcroft, J.L. (2010) Root growth patterns of perennial ryegrasses under well-watered and drought conditions, *New Zealand Journal of Agricultural Research*, 53(4), 377–388.

White, M.A., Nemani, R.R., Thornton, P.E. and Running, S.W. (2002) Satellite evidence of phenological differences between urbanized and rural areas of the eastern United States deciduous broadleaf forest, *Ecosystems*, 5(3), 260–273.

Zhang, F., Wang, C. and Wang, Z.-H. (2020) Response of natural vegetation to climate in dryland ecosystems: A comparative study between Xinjiang and Arizona, *Remote Sensing*, under review.

Zhou, X., Istanbulluoglu, E. and Vivoni, E.R. (2013) Modeling the ecohydrological role of aspect-controlled radiation on tree-grass-shrub coexistence in a semiarid climate, *Water Resources Research*, 49(5), 2872–2895.